

Influence of current mass on the spatially inhomogeneous chiral condensate

Shinji Maedan ¹

*Department of Physics, Tokyo National College of Technology, Kunugida-machi,
Hachioji, Tokyo 193-0997, Japan*

Abstract

It is known that, in the chiral limit, spatially inhomogeneous chiral condensate occurs in the Nambu-Jona-Lasinio (NJL) model at finite density within a mean-field approximation. We study here how an introduction of current quark mass affects the ground state with the spatially inhomogeneous chiral condensate. Numerical calculations show that, even if the current quark mass is introduced, the spatially inhomogeneous chiral condensate can take place. In order to obtain the ground state, the thermodynamic potential is calculated with a mean-field approximation. The influence of finite current mass on the thermodynamic potential consists of following two parts. One is a part coming from the field energy of the condensate, which favors inhomogeneous chiral condensate. The other is a part coming from the Dirac sea and the Fermi sea, which favors homogeneous chiral condensate. We also find that when the spatially inhomogeneous chiral condensate occurs, the baryon number density becomes spatially inhomogeneous.

¹ E-mail: maedan@tokyo-ct.ac.jp

1 Introduction

Quantum chromodynamics (QCD) at finite density is one of interesting topics in these days. The study of this field will help us to understand the physics of neutron stars, compact stars, and heavy ion collisions. In the vacuum state of QCD (quark chemical potential $\mu = 0$) at low temperature, the chiral symmetry is broken spontaneously and the confinement occurs. On the other hand, at extremely high densities (μ has very large values) and low temperature, color superconductivity will be realized in QCD [1, 2]. At such high density region, the perturbative calculation with the gauge coupling g is possible due to asymptotic freedom.

Now, at the moderate density region (moderate value of μ) where the coupling g is not small, how a ground state of QCD becomes? The method of perturbation of the coupling g cannot be used, and also it is difficult to apply the lattice QCD simulations to a system with finite density. Therefore, people have used effective theories of QCD such as the Nambu-Jona-Lasinio (NJL) model [3, 4] to study the physics at the moderate density region[5]. One of the interesting topics of these researches is that spatially inhomogeneous chiral condensate occurs in the ground state at the moderate density [6, 7, 15, 20].

Before discussing this topic in detail, let us look back the idea that fermionic condensate becomes spatially inhomogeneous at finite density. The possibility of spatially inhomogeneous chiral condensate in QCD at finite density was first discussed in Ref[8]. The authors in Ref[8] have shown that in the limit, N_c (number of colors) $\rightarrow \infty$, the spatially inhomogeneous chiral condensate occurs in the ground state of QCD at extremely high density region such that the relation $g^2 N_c \ll 1$ holds. That state is the standing wave ground state having the wave number 2μ , in which particle and hole with the same Fermi momentum \mathbf{p} ($|\mathbf{p}| = \mu$) condense (Overhauser effect [9]). When one takes the number of colors N_c of QCD to the realistic number three, however, it is shown by the later researches that the BCS effect (particle-particle condensation) is superior to the Overhauser effect (particle-hole condensation) and the color superconductor is realized at extremely high density [10, 11, 12]. In some two-dimensional models, it is argued that spatially inhomogeneous chiral condensate also occurs at finite density. In the chiral Gross-Neveu model with the limit $N \rightarrow \infty$ at finite density, it is shown that both scalar $\langle \bar{\psi}\psi \rangle$ and pseudoscalar $\langle \bar{\psi}i\gamma_5\psi \rangle$ become spatially inhomogeneous in the ground state ² [13, 14].

Now, let us return to the topic mentioned above. In Ref [6, 7], the NJL model with $N_c = 3$ and N_f (number of flavors) = 2 is considered at moderate density. Assuming the following mean-field,

$$\langle \bar{\psi}\psi \rangle = \Delta \cdot \cos(\mathbf{q} \cdot \mathbf{r}), \quad \langle \bar{\psi}i\gamma_5\tau_3\psi \rangle = \Delta \cdot \sin(\mathbf{q} \cdot \mathbf{r}), \quad (1)$$

² In the chiral Gross-Neveu model, finite bare quark mass case has also been studied [13]. When the bare quark mass is taken to be finite, the chiral angle depends on the value of the bare mass and the baryon density becomes spatially inhomogeneous.

where \mathbf{q} is a wave number vector, the authors in Ref [6, 7] obtain the ground state of that model by finding the minimum value of the thermodynamic potential in the mean-field approximation. In the chiral limit, they find numerically that the ground state has non-zero value of \mathbf{q} at low temperature and a high density region, namely spatially inhomogeneous dual chiral condensate, Eq.(1), occurs at that density region. Furthermore, the quark number density $\langle\psi^\dagger\psi\rangle$ becomes spatially homogeneous in the chiral limit.

In Ref [20], the $T - \mu$ phase diagram of the NJL-type model is studied around the chiral critical point in the chiral limit, which includes spatially inhomogeneous chiral condensate. There, the condensate is restricted to only scalar form instead of allowing both scalar and pseudoscalar form like Eq.(1). With more general ansatz for the scalar condensate, two phase transitions are found [20]. One is from the homogeneous massive phase to inhomogeneous phase, and the other is from the inhomogeneous phase to chirally symmetric phase, both of which are the second order. In the real world, however, the current quark mass is not zero and the pion (NG boson) has a mass of about 135MeV. Recently, the same issue is studied for the finite current quark mass [15]. In general, the thermodynamic potential Ω is a function of the complex order parameter $M(\mathbf{r})$,

$$M(\mathbf{r}) = m - 2G_s \left\{ \langle\bar{\psi}\psi\rangle + i\langle\bar{\psi}i\gamma_5\tau_3\psi\rangle \right\}, \quad (2)$$

and the stationary constraint, $\delta\Omega/\delta M(\mathbf{r})^* = 0$, is held in the ground state. In Ref [15], the stationary constraint is solved when the order parameter $M(\mathbf{r})$ is restricted to real (i.e., pseudoscalar condensate = 0). The numerical calculation using that real solution shows that the qualitative feature of the phase diagram remains unchanged. Now, how about the case where the order parameter $M(\mathbf{r})$ takes a complex value (i.e., both scalar and pseudoscalar condensate)? Unfortunately, it is very difficult to solve the stationary constraint with finite current mass when $M(\mathbf{r})$ is a complex value. Although no solution is known, we need to study the case where the order parameter $M(\mathbf{r})$ is complex by, for example, assuming ansatz for $M(\mathbf{r})$.

In this paper, we study the massive NJL model in the case where the order parameter is complex, that is, both scalar and pseudoscalar condensate exist. Concretely, we study how an introduction of finite current mass affects the ground state with the spatially inhomogeneous dual chiral condensate, Eq.(1), in Ref [6, 7]. Does the dual chiral condensate remain spatially inhomogeneous? And, does the quark number density remain spatially homogeneous? To find out these problems at moderate baryon density, we use the NJL model with finite current quark mass [15] (not the chiral limit case as in Ref [6, 7]). Here, let us compare the ansatz, Eq.(1), and that in Ref [20]. The ansatz, Eq.(1), allows the pseudoscalar condensate to occur in addition to the scalar condensate, while the ansatz in Ref [20] restricts the condensate to the scalar form. In this respect, we can say that Eq.(1) is more general than the ansatz in Ref [20]. On the other hand, concerning Fourier analysis of the assumed condensate, Eq.(1) is restricted to monochromatic wave, while the ansatz in Ref [20] contains various higher harmonics. From the viewpoint of this, we can say that the ansatz in Ref [20] is more general than

Eq.(1). Now, we return to the discussion of the NJL model. In the chiral limit, the thermodynamic potential can be calculated [6, 7] in a mean-field approximation under the assumption Eq.(1). On the other hand, when the current mass is taken to be finite, it is difficult to calculate the thermodynamic potential because the fermion propagator depends on the space coordinates \mathbf{r} explicitly. In order to avoid this difficulty, we will expand in powers of the current mass m . The thermodynamic potential ω will be calculated up to first order $O(m)$ and the ground state is obtained by finding a minimum value of ω .

This paper is organized as follows. The NJL model with $N_c = 3$ and $N_f = 2$ is introduced in section 2. We assume that mean fields $\langle \bar{\psi}\psi \rangle$ and $\langle \bar{\psi}i\gamma_5\tau_3\psi \rangle$, Eq.(1), exist at finite density, and the thermodynamic potential is calculated analytically in a mean-field approximation. In section 3, the numerical calculations of the thermodynamic potential at zero temperature are carried out and we obtain the ground state which minimize the thermodynamic potential. For a given quark chemical potential μ , these numerical calculations enable us to find whether the spatially inhomogeneous chiral condensate is realized ($\mathbf{q} \neq 0$) or not ($\mathbf{q} = 0$). In section 4, we show that the quark number density becomes spatially inhomogeneous when the spatially inhomogeneous chiral condensate is realized in the case of finite current quark mass. Section 5 is devoted to conclusions.

2 The Nambu-Jona-Lasinio model and standing wave ansatz

The Lagrangian of the NJL model is

$$\mathcal{L} = \bar{\psi}(i\cancel{\partial} - m)\psi + G \left[(\bar{\psi}\psi)^2 + (\bar{\psi}i\gamma_5\vec{\tau}\psi)^2 \right], \quad (3)$$

where the number of colors is $N_c = 3$ and the number of flavors is $N_f = 2$. Note that the current quark mass is taken to be finite and we set $m_u = m_d \equiv m > 0$. Now, we suppose the following mean fields exist at finite density [6, 7],

$$\langle \bar{\psi}\psi \rangle = C \cos(\mathbf{q} \cdot \mathbf{r}), \quad \langle \bar{\psi}i\gamma_5\tau_3\psi \rangle = C \sin(\mathbf{q} \cdot \mathbf{r}), \quad (C < 0), \quad (4)$$

where \mathbf{q} is the wave number vector and C is a constant. The other components are assumed to vanish, $\langle \bar{\psi}i\gamma_5\tau_1\psi \rangle = \langle \bar{\psi}i\gamma_5\tau_2\psi \rangle = 0$. When \mathbf{q} vanishes, these have the usual forms $\langle \bar{\psi}\psi \rangle = C$ and $\langle \bar{\psi}i\gamma_5\tau_3\psi \rangle = 0$. These mean fields are put on the chiral circle, $\langle \bar{\psi}\psi \rangle^2 + \langle \bar{\psi}i\gamma_5\tau_3\psi \rangle^2 = C^2$.

Here we shall make a comment on the ansatz Eq.(4). If the chiral limit, $m \rightarrow 0$, is considered, the bottom of the effective potential is the chiral circle, and it would be natural for $\langle \bar{\psi}\psi \rangle$ and $\langle \bar{\psi}i\gamma_5\tau_3\psi \rangle$ to be put on that chiral circle. However, when the current mass m is finite, the effective potential slightly tilts in the direction of $\bar{\psi}\psi$ and the shape of the effective potential becomes very complicated. In such case,

there might exist another ansatz which has more appropriate function of \mathbf{r} than the trigonometrical function used in Eq.(4). This point will be discussed in subsection 3.1 and section 5. In the present paper, we use the ansatz Eq.(4) for simplicity.

One can choose the direction of the wave number vector \mathbf{q} as $\mathbf{q} = (0, 0, q)$, ($q \geq 0$) without loss of generality. The mean-field approximated Lagrangian becomes

$$\mathcal{L}_{\text{MF}} = \bar{\psi} [i\cancel{\partial} - m + \mu \gamma_0 - M \exp(i\gamma_5 \tau_3 \mathbf{q} \cdot \mathbf{r})] \psi - \frac{M^2}{4G}, \quad (5)$$

where the parameter M has been defined as

$$M \equiv -2GC = 2G\sqrt{\langle \bar{\psi}\psi \rangle^2 + \langle \bar{\psi}i\gamma_5\tau_3\psi \rangle^2}, \quad (6)$$

and μ is the quark chemical potential. In the path integral representation, the bilinear form of fermion in \mathcal{L}_{MF} can be written as

$$\begin{aligned} & \int \mathcal{D}\bar{\psi} \mathcal{D}\psi \exp i \int d^4x \bar{\psi} [i\cancel{\partial} - m + \mu \gamma_0 - M \exp(i\gamma_5 \tau_3 \mathbf{q} \cdot \mathbf{r})] \psi \\ &= \int \mathcal{D}\bar{\psi}' \mathcal{D}\psi' \exp i \int d^4x \bar{\psi}' \left[i\gamma^\mu (\partial_\mu + \frac{i}{2}\gamma_5 \tau_3 q_\mu) - M + \mu \gamma_0 - m \exp(-i\gamma_5 \tau_3 \mathbf{q} \cdot \mathbf{r}) \right] \psi' \\ &= \int \mathcal{D}\bar{\psi}' \mathcal{D}\psi' \\ & \quad \times \exp i \int d^4x \bar{\psi}' \left[i\gamma^\mu (\partial_\mu + \frac{i}{2}\gamma_5 \tau_3 q_\mu) - M_t + \mu \gamma_0 - m \{ \exp(-i\gamma_5 \tau_3 \mathbf{q} \cdot \mathbf{r}) - 1 \} \right] \psi', \end{aligned} \quad (7)$$

where $\psi' \equiv \exp\left\{+\frac{i}{2}\gamma_5 \tau_3 \mathbf{q} \cdot \mathbf{r}\right\} \psi$ and $M + m \equiv M_t \geq m$. The propagator S of the field ψ' is

$$S = \frac{1}{i\gamma^\mu (\partial_\mu + \frac{i}{2}\gamma_5 \tau_3 q_\mu) - M_t + \mu \gamma_0 - m \{ \exp(-i\gamma_5 \tau_3 \mathbf{q} \cdot \mathbf{r}) - 1 \}}. \quad (8)$$

If the wave number vector \mathbf{q} vanishes, S represents a propagator of free fermion with a mass M_t .

When the wave number vector $\mathbf{q} \neq 0$ and the current quark mass $m \neq 0$, the denominator of the propagator S depends on the space coordinates \mathbf{r} explicitly, so that it becomes difficult to calculate the expression involving S . To avoid this difficulty, we separate S^{-1} into two,

$$S^{-1} = S_0^{-1} - V_m, \quad (9)$$

where

$$\begin{aligned} S_0^{-1} &\equiv i\gamma^\mu (\partial_\mu + \frac{i}{2}\gamma_5 \tau_3 q_\mu) - M_t + \mu \gamma_0, \\ V_m &\equiv m \{ \exp(-i\gamma_5 \tau_3 \mathbf{q} \cdot \mathbf{r}) - 1 \}. \end{aligned} \quad (10)$$

Using the identity

$$\frac{1}{A} - \frac{1}{B} = \frac{1}{B}(B - A)\frac{1}{A}, \quad (11)$$

for any noncommutable operators A and B , we obtain

$$S = S_0 + S_0 V_m S. \quad (12)$$

From this equation, we have

$$S = S_0 + S_0 V_m S_0 + S_0 V_m S_0 V_m S_0 + \dots \quad (13)$$

Here, it should be noted that in the chiral limit, $m \rightarrow 0$, we have, $V_m \rightarrow 0$. Since the current quark mass m is the smallest energy scale in the system, we treat the $V_m \sim O(m)$ as perturbative part and neglect higher order $O(V_m^2)$. We shall use the approximate equation (13) to calculate the expression involving S , as will be done in section 4. For the expression involving S^{-1} , the separation Eq.(9) will be used as follows.

The thermodynamic potential ω is useful so as to find the ground state of the system with finite density $\mu \geq 0$ and finite temperature $T \geq 0$. In the imaginary time formulation [16], $\tau = it$, the mean-field approximated thermodynamic potential ω has the form,

$$\begin{aligned} \omega &= -\frac{T}{V} \ln N' \int \mathcal{D}\bar{\psi} \mathcal{D}\psi \exp \int_0^\beta d\tau \int d^3x \mathcal{L}_{\text{MF}} \\ &= \frac{M^2}{4G} - \frac{T}{V} \ln \int \mathcal{D}\bar{\psi}' \mathcal{D}\psi' \exp \int_0^\beta d\tau \int d^3x \bar{\psi}' S^{-1} \psi'. \end{aligned} \quad (14)$$

Here $V = L^3$ is the volume, β is $1/T$, and the irrelevant constant is omitted. Since the path integral calculation in Eq.(14) is difficult, we regard the term V_m in Eq.(9) as perturbative part and obtain ω up to the order $O(V_m)$. We separate the action $\int_0^\beta d\tau \int d^3x \bar{\psi}' S^{-1} \psi' \equiv A$ into two parts referring to Eq.(9),

$$A = A_0 + A_m. \quad (15)$$

Here, A_0 and A_m are

$$\begin{aligned} A_0 &\equiv \int_0^\beta d\tau \int d^3x \bar{\psi}' S_0^{-1} \psi', \\ A_m &\equiv \int_0^\beta d\tau \int d^3x \bar{\psi}' (-V_m) \psi', \end{aligned} \quad (16)$$

and note that in the chiral limit, $m \rightarrow 0$, one has, $A_m \rightarrow 0$. Expanding $\exp(A_m)$, we have

$$\begin{aligned} w &= \frac{M^2}{4G} - \frac{T}{V} \ln \int \mathcal{D}\bar{\psi}' \mathcal{D}\psi' \exp A \\ &= \frac{M^2}{4G} - \frac{T}{V} \ln \int \mathcal{D}\bar{\psi}' \mathcal{D}\psi' \exp(A_0) \sum_{l=0}^{\infty} \frac{1}{l!} A_m^l \\ &= \frac{M^2}{4G} - \frac{T}{V} \left[\ln \int \mathcal{D}\bar{\psi}' \mathcal{D}\psi' \exp(A_0) + \frac{\int \mathcal{D}\bar{\psi}' \mathcal{D}\psi' A_m \exp(A_0)}{\int \mathcal{D}\bar{\psi}' \mathcal{D}\psi' \exp(A_0)} + O(V_m^2) \right]. \end{aligned} \quad (17)$$

The leading term in Eq.(17) is

$$\begin{aligned}
-\frac{T}{V} \ln \int \mathcal{D} \bar{\psi}' \mathcal{D} \psi' \exp(A_0) &= -\frac{T}{V} N_c \ln \text{Det} \left(\frac{S_0^{-1}}{T} \right) \\
&= -TN_c \int \frac{d^3 p}{(2\pi)^3} \sum_{j=-\infty}^{\infty} \ln \det \left(\frac{S_0^{-1}}{T} \right) \\
&\equiv \omega_D + \omega_F,
\end{aligned} \tag{18}$$

where

$$S_0 = \frac{1}{\gamma^\mu p_\mu - M_t - \frac{1}{2} \gamma^\mu q_\mu \gamma_5 \tau_3}, \quad (p^0 = i\omega_j + \mu = i(2j+1)\pi T + \mu). \tag{19}$$

The propagator S_0 has four energy poles, $p_0 = \epsilon_n (n = 1, 2, 3, 4)$, with

$$\begin{aligned}
\epsilon_1 = \epsilon_- &= \sqrt{p_\perp^2 + \left(\sqrt{M_t^2 + p_z^2} - \frac{q}{2} \right)^2} > 0, \\
\epsilon_2 = \epsilon_+ &= \sqrt{p_\perp^2 + \left(\sqrt{M_t^2 + p_z^2} + \frac{q}{2} \right)^2} > 0, \\
\epsilon_3 &= -\epsilon_1, \\
\epsilon_4 &= -\epsilon_2.
\end{aligned} \tag{20}$$

The ω_D and ω_F have the form [6, 7],

$$\begin{aligned}
\omega_D \equiv -N_c N_f \int \frac{d^3 p}{(2\pi)^3} &\left[(\epsilon_1 + \epsilon_2) + T \ln \left(1 + \exp \left\{ -\frac{(\epsilon_1 + \mu)}{T} \right\} \right) \right. \\
&\quad \left. + T \ln \left(1 + \exp \left\{ -\frac{(\epsilon_2 + \mu)}{T} \right\} \right) \right],
\end{aligned} \tag{21}$$

$$\begin{aligned}
\omega_F \equiv -N_c N_f \int \frac{d^3 p}{(2\pi)^3} &\left[T \ln \left(1 + \exp \left\{ -\frac{(\epsilon_1 - \mu)}{T} \right\} \right) \right. \\
&\quad \left. + T \ln \left(1 + \exp \left\{ -\frac{(\epsilon_2 - \mu)}{T} \right\} \right) \right].
\end{aligned} \tag{22}$$

The ω_D represents the contribution from the Dirac sea and ω_F the contribution from the Fermi sea. The next leading order of $O(V_m)$ is [16]

$$\begin{aligned}
&-\frac{T}{V} \frac{\int \mathcal{D} \bar{\psi}' \mathcal{D} \psi' A_m \exp(A_0)}{\int \mathcal{D} \bar{\psi}' \mathcal{D} \psi' \exp(A_0)} \\
&= -\frac{T}{V} N_c (-1) m \left\{ \frac{\sin(Lq/2)}{(Lq/2)} - 1 \right\} V \sum_{j=-\infty}^{\infty} \int \frac{d^3 p}{(2\pi)^3} \text{tr} S_0 \\
&\equiv \delta\omega_D + \delta\omega_F,
\end{aligned} \tag{23}$$

where [17]

$$\begin{aligned}\delta\omega_{\text{D}} &\equiv \left\{ \frac{\sin(Lq/2)}{(Lq/2)} - 1 \right\} m N_c N_f \int \frac{d^3p}{(2\pi)^3} \\ &\quad \times \left[\sum_{n=3,4} \frac{M_t \left\{ \sqrt{M_t^2 + p_z^2} + (-1)^n \left(\frac{q}{2}\right) \right\}}{\epsilon_n \sqrt{M_t^2 + p_z^2}} \left(1 + \exp \left\{ \frac{(\epsilon_n - \mu)}{T} \right\} \right)^{-1} \right] \\ &= \left\{ \frac{\sin(Lq/2)}{(Lq/2)} - 1 \right\} m \frac{\partial}{\partial M_t} \omega_{\text{D}},\end{aligned}\quad (24)$$

$$\begin{aligned}\delta\omega_{\text{F}} &\equiv \left\{ \frac{\sin(Lq/2)}{(Lq/2)} - 1 \right\} m N_c N_f \int \frac{d^3p}{(2\pi)^3} \\ &\quad \times \left[\sum_{n=1,2} \frac{M_t \left\{ \sqrt{M_t^2 + p_z^2} + (-1)^n \left(\frac{q}{2}\right) \right\}}{\epsilon_n \sqrt{M_t^2 + p_z^2}} \left(1 + \exp \left\{ \frac{(\epsilon_n - \mu)}{T} \right\} \right)^{-1} \right] \\ &= \left\{ \frac{\sin(Lq/2)}{(Lq/2)} - 1 \right\} m \frac{\partial}{\partial M_t} \omega_{\text{F}}.\end{aligned}\quad (25)$$

Both $\delta\omega_{\text{D}}$ and $\delta\omega_{\text{F}}$ vanish in the chiral limit,

$$\lim_{m \rightarrow 0} \delta\omega_{\text{D}} = \lim_{m \rightarrow 0} \delta\omega_{\text{F}} = 0, \quad (26)$$

as well as in the limit, $q \rightarrow 0$, as it should be.

Eventually, thermodynamic potential ω up to $O(V_m)$ becomes

$$\omega = \omega_{\text{D}} + \omega_{\text{F}} + \frac{(M_t - m)^2}{4G} + \delta\omega_{\text{D}} + \delta\omega_{\text{F}} + O(V_m^2), \quad (27)$$

where $\delta\omega_{\text{D}}$ and $\delta\omega_{\text{F}}$ come from the term, V_m . In the zero temperature limit, $T \rightarrow 0$, each term becomes

$$\omega_{\text{D}} = -N_c N_f \int \frac{d^3p}{(2\pi)^3} (\epsilon_1 + \epsilon_2), \quad (28)$$

$$\omega_{\text{F}} = -N_c N_f \int \frac{d^3p}{(2\pi)^3} [(\mu - \epsilon_1) \theta(\mu - \epsilon_1) + (\mu - \epsilon_2) \theta(\mu - \epsilon_2)], \quad (29)$$

$$\delta\omega_{\text{D}} = \left\{ \frac{\sin(Lq/2)}{(Lq/2)} - 1 \right\} m \frac{\partial}{\partial M_t} \omega_{\text{D}}, \quad (30)$$

$$\delta\omega_{\text{F}} = \left\{ \frac{\sin(Lq/2)}{(Lq/2)} - 1 \right\} m \frac{\partial}{\partial M_t} \omega_{\text{F}}. \quad (31)$$

Note that ω_{F} is always negative, $\omega_{\text{F}} \leq 0$. But $\delta\omega_{\text{F}}$ can have either positive or negative value.

3 Numerical calculation with zero temperature

When the values of chemical potential μ and temperature T are given, the ground state of our system can be described by two parameters (M_t, q) which minimize the thermodynamic potential ω . We will obtain the ground state in the zero temperature case $T = 0$ by numerical calculations. Because the NJL model is a cut-off theory, a regularization method should be specified to define the theory, and we utilize the proper-time regularization method [18] here. With the proper-time regularization, ω_D has the following form [6, 7],

$$\omega_D = N_c N_f \frac{1}{4\pi^{3/2}} \int_0^\infty \frac{dk_z}{2\pi} \int_{1/\Lambda^2}^\infty \frac{d\tau}{\tau^{5/2}} \left[\exp \left\{ - \left(\sqrt{k_z^2 + M_t^2} - \frac{q}{2} \right)^2 \tau \right\} + \exp \left\{ - \left(\sqrt{k_z^2 + M_t^2} + \frac{q}{2} \right)^2 \tau \right\} \right], \quad (32)$$

where Λ is a cut-off parameter. The regularized $\delta\omega_D$ can be obtained from Eq.(32) by use of Eq.(24).

We now set the three input parameters (G, m, Λ) so that the observed values $f_\pi = 92.4$ MeV and $m_\pi = 135$ MeV are reproduced in the vacuum state $\mu = 0$. We first give arbitrary values of Λ , and then fix G and m so as to suit f_π and m_π to their observed values. In Appendix A, the way of determining (G, m, Λ) is given in detail. There still remains one degree of freedom, because we use only two observable quantities f_π and m_π to determine the three input parameters. Therefore, we require further that the chiral phase transition should be first order in spatially homogeneous case ($q = 0$) at finite density. The parameters (G, m, Λ) obtained in Appendix A are restricted by this requirement. The spatially homogeneous case ($q = 0$) will be considered in the next subsection.

3.1 Spatially homogeneous case at finite density

Before studying spatially inhomogeneous case ($q \neq 0$), we consider in this subsection spatially homogeneous case ($q = 0$), which is easier to deal with. As is well known [19], chiral symmetry is restored as the quark chemical potential μ increases (density increases). Here we restrict the values (G, m, Λ) obtained in Appendix A by requiring the chiral phase transition to be first order when $q = 0$. For a given value of μ (and $T = 0$), the ground state is described by the parameter M_t which minimize the thermodynamic potential ω . By the numerical calculations, we find that the chiral phase transition becomes first order when the input parameters (G, m, Λ) obtained in Appendix A satisfy the following relation,

$$G\Lambda^2 \geq 5.6. \quad (33)$$

Henceforth, we use the input parameters' values (G, m, Λ) obtained in Appendix A which also satisfy the condition Eq.(33).

In analyzing the behavior of M_t , we find the following by numerical calculations. As the chemical potential μ increases, the parameter M_t decreases discontinuously and the first order phase transition of chiral symmetry occurs. If μ increases further ($\mu \leq \Lambda$), one might expect that the parameter M_t will decrease more and approach m , $M_t > m$. However, our observation is that, after chiral phase transition, M_t decreases more and eventually it becomes $M_t < m$ when μ exceeds about 0.7Λ . The relation $M_t < m$ implies that the dynamically obtained quark mass M_t is less than the current quark mass if $\mu \gtrsim 0.7\Lambda$, and this phenomenon is unnatural. Hence we restrict ourselves to the region, $\mu \lesssim 0.7\Lambda$ and do not consider the value of μ larger than 0.7Λ . The fact that the relation $M_t < m$ holds in the region $\mu \gtrsim 0.7\Lambda$ will be caused by our choice of the regularization method, that is the proper-time regularization. This point will be discussed in Appendix B.

Before closing this subsection, we would like to study the effects of current mass on the spatially homogeneous chiral condensate. This search would be helpful to investigate the effects of current mass on the spatially inhomogeneous chiral condensate which will be discussed in section 3.3. In the ansatz, Eq.(4), when the chiral condensates are spatially homogeneous ($q = 0$), the condensates are chosen to be $\langle \bar{\psi}\psi \rangle = C$ and $\langle \bar{\psi}i\gamma_5\tau_3\psi \rangle = 0$. In the spatially homogeneous case, it is known that this choice realizes the lowest value of the energy if the current quark mass is finite. Here, we make sure of this fact by the thermodynamic potential ω expanded in V_m . To this end, we assume in this subsection the following spatially homogeneous chiral condensate,

$$\langle \bar{\psi}\psi \rangle = C \cos \phi, \quad \langle \bar{\psi}i\gamma_5\tau_3\psi \rangle = C \sin \phi, \quad (C < 0), \quad (34)$$

where the chiral angle ϕ is a constant ($0 \leq \phi < 2\pi$). The thermodynamic potential having these condensates can be calculated as done in Section 2,

$$\omega = \left\{ \omega_D + \omega_F + \frac{M_t^2}{4G} \right\} + \left\{ -\frac{m}{2G}M_t + \delta\omega_D + \delta\omega_F + \frac{m^2}{4G} \right\} + O(V_m^2), \quad (35)$$

where $V_m = m \{ \exp(-i\gamma_5\tau_3\phi) - 1 \}$. Each term has the following form,

$$\omega_D = -N_c N_f \int \frac{d^3p}{(2\pi)^3} 2 \sqrt{\mathbf{p}^2 + M_t^2}, \quad (36)$$

$$\omega_F = -N_c N_f \int \frac{d^3p}{(2\pi)^3} 2 \left(\mu - \sqrt{\mathbf{p}^2 + M_t^2} \right) \theta \left(\mu - \sqrt{\mathbf{p}^2 + M_t^2} \right), \quad (37)$$

$$\begin{aligned} \delta\omega_D &= (\cos \phi - 1) m (-1) N_c N_f \int \frac{d^3p}{(2\pi)^3} 2 \frac{M_t}{\sqrt{\mathbf{p}^2 + M_t^2}} \\ &= (\cos \phi - 1) m \frac{\partial}{\partial M_t} \omega_D, \end{aligned} \quad (38)$$

$$\begin{aligned} \delta\omega_F &= (\cos \phi - 1) m N_c N_f \int \frac{d^3p}{(2\pi)^3} 2 \frac{M_t}{\sqrt{\mathbf{p}^2 + M_t^2}} \theta \left(\mu - \sqrt{\mathbf{p}^2 + M_t^2} \right) \\ &= (\cos \phi - 1) m \frac{\partial}{\partial M_t} \omega_F. \end{aligned} \quad (39)$$

Thermodynamic potential ω is regarded as a function of two variables, (M_t, ϕ) , and the ground state is described by (M_t, ϕ) which minimize ω . Since the ω depends on the chiral angle through $\cos \phi$, one can constraint the chiral angle, $0 \leq \phi \leq \pi$. The part, $\{\omega_D + \omega_F + M_t^2/4G\}$, in Eq.(35) does not depend on ϕ . The terms which represent the current mass effects are $\{-(m/2G)M_t + \delta\omega_D + \delta\omega_F\}$ (the term, $m^2/4G$, can be regarded as a constant because it does not depend on M_t and ϕ). The term, $-(m/2G)M_t$, depends on only M_t , and this term lowers ω . Next, the term, $\delta\omega_D$, takes positive value, $\delta\omega_D \geq 0$. This $\delta\omega_D$ is a monotone increasing function of the chiral angle ϕ in the range of $0 \leq \phi \leq \pi$, therefore the term, $\delta\omega_D$, tends to move the chiral angle ϕ closer to the value zero. Thirdly, the term, $\delta\omega_F$, vanishes if $\mu \leq M_t$, whereas it takes negative value $\delta\omega_F < 0$ if $\mu > M_t$. This $\delta\omega_F$ is a monotone decreasing function of ϕ in the range of $0 \leq \phi \leq \pi$. Therefore the term, $\delta\omega_F$, tends to move ϕ closer to the value π , and this tendency rises when the chemical potential μ becomes larger. We can say that the term $\delta\omega_D$ and the term $\delta\omega_F$ compete. Then, how about their sum, $(\delta\omega_F + \delta\omega_D)$? The regularized $\delta\omega_D$ is obtained from Eq.(32) by use of Eq.(38), and the sum is

$$\begin{aligned} \delta\omega_F + \delta\omega_D = & (\cos \phi - 1) 2 m N_c N_f M_t (-1) \\ & \times \left[\frac{1}{8\pi^2} \int_{1/\Lambda^2}^{\infty} d\tau \frac{1}{\tau^2} e^{-M_t^2 \tau} - \int \frac{d^3 p}{(2\pi)^3} \frac{1}{\sqrt{\mathbf{p}^2 + M_t^2}} \theta \left(\mu - \sqrt{\mathbf{p}^2 + M_t^2} \right) \right] \end{aligned} \quad (40)$$

The equation enclosed in the brackets of the right-handed side is the same with that in the brackets in Eq.(B.1). This equation takes positive value when $0 \leq \mu < \mu_c$, and becomes zero if $\mu = \mu_c$, as is discussed in Appendix B. The equation is a monotone decreasing function of μ . Here, μ_c is defined in Eq.(B.2) and takes the value, $\mu_c \approx 0.7\Lambda$ if $M_t/\Lambda \ll 1$. The sum, $(\delta\omega_F + \delta\omega_D)$, is then a monotone increasing function of ϕ in the range of $0 \leq \mu < \mu_c$. We therefore conclude that, in the range of $0 \leq \mu < \mu_c$, $(\delta\omega_F + \delta\omega_D)$ tends to move the chiral angle ϕ closer to the value zero, and this tendency becomes weaker when μ grows. From the above, we have shown that, in the range of $0 \leq \mu < \mu_c$, the condensate, $\langle \bar{\psi}\psi \rangle = C$, $\langle \bar{\psi}i\gamma_5\tau_3\psi \rangle = 0$, realizes the lowest value of the thermodynamic potential ω if the chiral condensate is restricted to be spatially homogeneous.

The foregoing computation helps us discuss qualitatively the appropriateness of the ansatz Eq.(4) which we put for the spatially inhomogeneous chiral condensate. When μ takes the value zero, the above computation concerning the spatially homogeneous condensate shows that the ω does depend on the chiral angle ϕ and one cannot ignore that dependence. Then Eq.(4) would not be appropriate if μ has small value because $\langle \bar{\psi}\psi \rangle$ and $\langle \bar{\psi}i\gamma_5\tau_3\psi \rangle$ are put on the chiral circle in Eq.(4). On the other hand, the dependence of ω on ϕ becomes weaker when the value of μ becomes larger. Therefore we expect that the ansatz putting $\langle \bar{\psi}\psi \rangle$ and $\langle \bar{\psi}i\gamma_5\tau_3\psi \rangle$ on the chiral circle such as Eq.(4) is a moderate assumption when μ takes large value if we neglect the contribution of order $O(V_m^2)$.

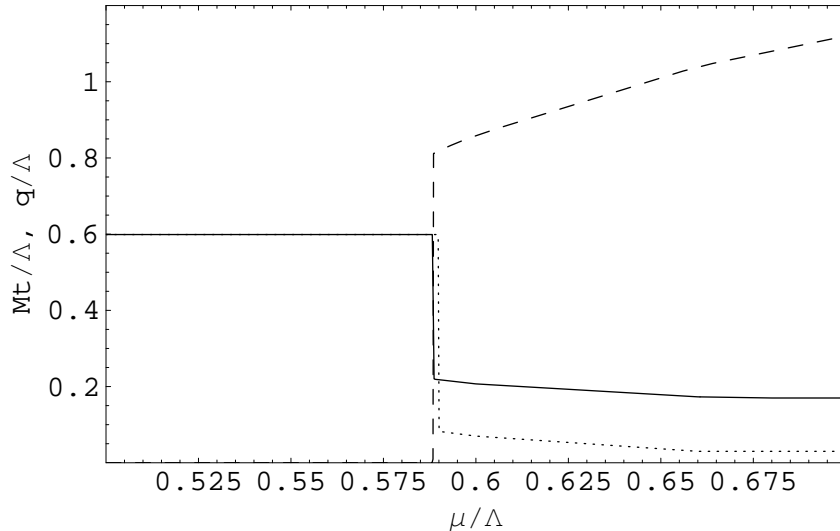


Figure 1: The mass M_t (solid) and the wave number q (long-dashed) as a function of the chemical potential μ , in units of Λ . For comparison, $M_t(q=0)$ without inhomogeneous chiral condensate is also represented by dotted line.

3.2 Numerical results

As is discussed in the previous subsection, we restrict ourselves to the following region,

$$G\Lambda^2 \geq 5.6, \quad \mu \lesssim 0.7\Lambda, \quad (41)$$

the first condition comes from the requirement that the chiral phase transition is first order when $q=0$, and the second comes from the requirement that the dynamically obtained mass M_t is not less than the current quark mass m when $q=0$. The parameter L is taken to be a enough large value, $L = 2 \times 10^8 / \Lambda$. For a given value of μ , the ground state is obtained by determining two values (M_t, q) which minimize the thermodynamic potential ω . If $q=0$ is the solution which minimizes ω , the chiral condensate is spatially homogeneous. On the other hand, if $q \neq 0$ is the solution which minimizes ω , the chiral condensate is spatially inhomogeneous. According to numerical calculations, we always have the solution $q=0$ for arbitrary values of μ when $5.6 \leq G\Lambda^2 < 6.94$. Namely, in the region $5.6 \leq G\Lambda^2 < 6.94$, the ground state is not spatially inhomogeneous chiral condensate.

If $G\Lambda^2$ is larger than 6.94, $G\Lambda^2 \geq 6.94$, however, there exist the solutions $q \neq 0$ for large values of μ . Here we show a concrete example of numerical results with the input parameters, $G\Lambda^2 = 7.513$, $\Lambda = 635\text{MeV}$, and $m = 15.3\text{MeV}$, ($M_t(\mu=0) = 380\text{MeV}$) in Figure.1. In the low density region, $0 \leq \mu < 0.5885\Lambda$, we have $q=0$ and the chiral condensate is spatially homogeneous as usual. In the high density region, $0.5885\Lambda \leq \mu \leq 0.7\Lambda$, we get $q \neq 0$ (long-dashed line) and spatially inhomogeneous dual chiral condensate is realized. Let us see the behavior of M_t represented by solid line.

Since M_t decreases discontinuously at $\mu = 0.5885\Lambda$, the chiral phase transition is first order. In this high density region, $\mu \geq 0.5885\Lambda$, one finds by numerical calculations that the relation, $\mu < M_t + q/2$, holds. Therefore, the ϵ_2 state is occupied with no quark because of $\epsilon_2 \geq M_t + q/2$, and all quarks in the Fermi sea are filled in the ϵ_1 states. For comparison, we also show a local minimum solution $M_t(q = 0)$ with $q = 0$, which is represented by dotted line in Figure.1. In the region, $\mu \geq 0.5885\Lambda$, the points (M_t (solid line), $q \neq 0$ (long - dashed line)) in the $M_t - q$ plane correspond to the absolute minimum energy state (ground state) of ω , and the points (M_t (dotted line), $q = 0$) correspond to the local minimum energy state. The spatially inhomogeneous ($q \neq 0$) dual chiral condensate occurs at densities higher than about the usual ($q = 0$) chiral phase transition point, $\mu = 0.59\Lambda$. The characteristic feature in Figure.1 is as follows. As the chemical potential μ increases over the value of 0.5885Λ , M_t decreases a little. Even at high density of $\mu = 0.7\Lambda$, the value of M_t remains rather large, $M_t \approx 0.17\Lambda$. This feature is different from the result obtained in the chiral limit case [6, 7]. If $G\Lambda^2$ takes the values, $7.04 \leq G\Lambda^2 \leq 8.1$, the behavior of $q(M_t)$ in the $q - \mu$ plane (in the $M_t - \mu$ plane) is similar to that in Figure.1. On the other hand, if $G\Lambda^2$ takes the values, $6.94 \leq G\Lambda^2 < 7.04$, the wave number q remains zero at the value of chemical potential μ_{chi} at which M_t decreases discontinuously. The wave number q becomes non-zero at the value of the chemical potential whose magnitude is over μ_{chi} .

3.3 Effects of current mass

In this subsection, the effect of current mass on the thermodynamic potential ω , Eq.(27), with $T = 0$ is cleared. We divide ω into two parts,

$$\omega = \left\{ \omega_{\text{D}} + \omega_{\text{F}} + \frac{M_t^2}{4G} \right\} + \left\{ -\frac{m}{2G} M_t + (\delta\omega_{\text{D}} + \delta\omega_{\text{F}}) + \frac{m^2}{4G} \right\} + O(V_m^2). \quad (42)$$

The thermodynamic potential ω is regarded as a function of the two parameters (M_t, q). The terms $\delta\omega_{\text{D}}$ and $\delta\omega_{\text{F}}$ are defined in Eq.(24) and (25), and the effects of current mass m is described by the second brackets of Eq.(42). Because the ground state is described by the two parameters (M_t, q) which minimize ω , the term $m^2/4G$ in the second brackets of Eq.(42) can be regarded as a constant. We then need to see remaining two terms, $-(m/2G)M_t$ and $(\delta\omega_{\text{D}} + \delta\omega_{\text{F}})$. First, the term $-(m/2G)M_t$ in the second brackets of Eq.(42) depends on M_t , not on q . The larger M_t is, the more markedly this term $-(m/2G)M_t$ lowers ω independently of q . Therefore, the term $-(m/2G)M_t$ has possibility to make ω have minimum value at the point $q \neq 0$.

Second, let us inspect the term $(\delta\omega_{\text{D}} + \delta\omega_{\text{F}})$. We want to judge whether $\delta\omega_{\text{D}}$ and $\delta\omega_{\text{F}}$ tend to make ω minimized at the point $q \neq 0$ or not. To this end, the dependence of $\delta\omega_{\text{D}}$ ($\delta\omega_{\text{F}}$) on q is found by expanding $\delta\omega_{\text{D}}$ ($\delta\omega_{\text{F}}$) about $q = 0$,

$$\delta\omega_{\text{D}} = \frac{1}{2!} \left. \frac{\partial^2(\delta\omega_{\text{D}})}{\partial q^2} \right|_{q=0} \cdot q^2 + O(q^3). \quad (43)$$

Since the coefficient of q^2 ,

$$\frac{1}{2!} \frac{\partial^2(\delta\omega_{\text{D}})}{\partial q^2} \Big|_{q=0} = \frac{1}{6} \left(\frac{L}{2}\right)^2 m N_c N_f \frac{M_t}{4\pi^2} \int_{1/\Lambda^2}^{\infty} d\tau \frac{1}{\tau^2} e^{-M_t^2 \tau} > 0, \quad (44)$$

is positive, the value of $\delta\omega_{\text{D}}$ at $q \neq 0$ is larger than that at $q = 0$ when q is small. Hence, $\delta\omega_{\text{D}}$ tends to make ω not minimized at the point $q \neq 0$ if q is small. Similarly, $\delta\omega_{\text{F}}$ is expanded about $q = 0$,

$$\delta\omega_{\text{F}} = \frac{1}{2!} \frac{\partial^2(\delta\omega_{\text{F}})}{\partial q^2} \Big|_{q=0} \cdot q^2 + O(q^3). \quad (45)$$

Since the coefficient of q^2 ,

$$\frac{1}{2!} \frac{\partial^2(\delta\omega_{\text{F}})}{\partial q^2} \Big|_{q=0} = -\frac{1}{6} \left(\frac{L}{2}\right)^2 m N_c N_f \cdot 2M_t \int \frac{d^3p}{(2\pi)^3} \frac{1}{\epsilon} \theta(\mu - \epsilon) < 0, \quad (46)$$

is negative, the value of $\delta\omega_{\text{F}}$ at $q \neq 0$ is smaller than that at $q = 0$ when q is small. Hence, $\delta\omega_{\text{F}}$ tends to make ω minimized at the point $q \neq 0$ if q is small. Now, how about the sum, $(\delta\omega_{\text{D}} + \delta\omega_{\text{F}})$? Expanding $(\delta\omega_{\text{D}} + \delta\omega_{\text{F}})$ about $q = 0$, we obtain

$$\delta\omega_{\text{D}} + \delta\omega_{\text{F}} = \frac{1}{2!} \frac{\partial^2(\delta\omega_{\text{D}} + \delta\omega_{\text{F}})}{\partial q^2} \Big|_{q=0} \cdot q^2 + O(q^3), \quad (47)$$

where the coefficient of q^2 is

$$\frac{1}{6} \left(\frac{L}{2}\right)^2 2 m N_c N_f M_t \left[\frac{1}{8\pi^2} \int_{1/\Lambda^2}^{\infty} d\tau \frac{1}{\tau^2} e^{-M_t^2 \tau} - \int \frac{d^3p}{(2\pi)^3} \frac{1}{\epsilon} \theta(\mu - \epsilon) \right]. \quad (48)$$

The equation enclosed in the above brackets is the same with the equation in the brackets in Eq.(B.1), which equation takes positive value when $\mu \leq \mu_c (\approx 0.7\Lambda)$, as is discussed in Appendix B. The coefficient Eq.(48) is positive if $\mu \leq \mu_c (\approx 0.7\Lambda)$. We can say that when q is small the value of $(\delta\omega_{\text{D}} + \delta\omega_{\text{F}})$ at $q \neq 0$ is larger than that at $q = 0$. Furthermore, we confirm by numerical calculations that $(\delta\omega_{\text{D}} + \delta\omega_{\text{F}})$ takes positive value in the range of $0 \leq q \leq 2\mu$ when $\mu \leq 0.7\Lambda$. Eventually, we find that $(\delta\omega_{\text{D}} + \delta\omega_{\text{F}})$ tends to make ω not minimized at the point $q \neq 0$. In other words, $(\delta\omega_{\text{D}} + \delta\omega_{\text{F}})$ tends not to realize the inhomogeneous chiral condensate ($q \neq 0$).

Our argument in this subsection is summarized as follows. The influence of the current mass m on the thermodynamic potential ω is represented as $-(m/2G)M_t + (\delta\omega_{\text{D}} + \delta\omega_{\text{F}})$. The term $-(m/2G)M_t$ tends to make ω minimized at the point $q \neq 0$. On the other hand, the term $(\delta\omega_{\text{D}} + \delta\omega_{\text{F}})$ tends to make ω not minimized at the point $q \neq 0$. Whether the introduction of the finite current mass tends to materialize the inhomogeneous chiral condensate ($q \neq 0$) or not depends on the competition between the term $-(m/2G)M_t$ and the term $(\delta\omega_{\text{D}} + \delta\omega_{\text{F}})$.

4 Spatially inhomogeneous baryon density

In the previous subsection, we consider the effect of the finite current mass on the ground state with the spatially inhomogeneous chiral condensate. The influence of the current mass on the thermodynamic potential is represented as $-(m/2G)M_t + (\delta\omega_D + \delta\omega_F)$. There is, however, another influence which the current mass has on the system. In the chiral limit, the baryon density is spatially homogeneous even if the spatially inhomogeneous chiral condensate occurs [6, 7]. In contrast, when the current mass is finite, the baryon density becomes spatially inhomogeneous if the spatially inhomogeneous chiral condensate occurs. This will be shown as follows.

The quark number (one-thirds of the baryon number) density ρ can be written by the field ψ' defined in section 2,

$$\begin{aligned}
\rho &= \langle \psi^\dagger \psi \rangle \\
&= \langle \psi'^\dagger \psi' \rangle \\
&= -i \operatorname{tr} [\gamma^0 S(x, x)] \\
&= -i \operatorname{tr} [\gamma^0 S_0(x, x)] - i \int d^4 y \operatorname{tr} [\gamma^0 S_0(x, y) V_m(y) S_0(y, x)] + O(V_m^2) \\
&= -i \left(iT \sum_{j=-\infty}^{\infty} \int \frac{d^3 p}{(2\pi)^3} \right) \operatorname{tr} [\gamma^0 S_0(p)] \\
&\quad - im \left\{ - \left(iT \sum_{j=-\infty}^{\infty} \int \frac{d^3 p}{(2\pi)^3} \right) \operatorname{tr} [\gamma^0 S_0(p) S_0(p)] \right. \\
&\quad \quad + \exp(-i\mathbf{q} \cdot \mathbf{r}) \left(iT \sum_{j=-\infty}^{\infty} \int \frac{d^3 p}{(2\pi)^3} \right) \operatorname{tr} \left[\gamma^0 S_0(p) \frac{(1 + \gamma_5 \tau_3)}{2} S_0(p + q) \right] \\
&\quad \quad \left. + \exp(i\mathbf{q} \cdot \mathbf{r}) \left(iT \sum_{j=-\infty}^{\infty} \int \frac{d^3 p}{(2\pi)^3} \right) \operatorname{tr} \left[\gamma^0 S_0(p) \frac{(1 - \gamma_5 \tau_3)}{2} S_0(p - q) \right] \right\} \\
&\quad + O(V_m^2), \tag{49}
\end{aligned}$$

where S is the propagator of ψ' , and the perturbative approximation Eq.(13) has been used. Since ρ depends on \mathbf{r} , the baryon number density is spatially inhomogeneous. The wave number representing inhomogeneous of baryon number density coincides with that of chiral condensate up to the order $O(V_m)$. In the chiral limit, the baryon number density becomes spatially homogeneous, indeed. Why does the baryon number density become spatially inhomogeneous when the current mass is finite? The path integral representation Eq.(7) will help us to see this. The propagator of the field ψ depends on the space coordinates \mathbf{r} explicitly. In the chiral limit, however, the propagator S of the field ψ' introduced in Eq.(7) does not depend on \mathbf{r} . One can write ρ in terms of the propagator S in the mean-field approximation. On the other hand, when the current mass is finite, the propagator S does depend on \mathbf{r} explicitly.

5 Conclusion

We have studied how the introduction of finite current quark mass affects the ground state with the spatially inhomogeneous chiral condensate, Eq.(4), which is actually realized in the NJL model at finite density in the chiral limit. Our numerical calculations show that, even if the finite current quark mass is introduced, the spatially inhomogeneous chiral condensate can take place. If $G\Lambda^2 \geq 6.94$ is satisfied, the spatially inhomogeneous chiral condensate occurs (i.e., $q \neq 0$) at high density. When $5.6 \leq G\Lambda^2 < 6.94$, the spatially inhomogeneous chiral condensate does not occur (i.e., $q = 0$). The ground state was determined by obtaining the values of two parameters (M_t, q) which minimize the thermodynamic potential ω . When the current mass m takes a finite small value, the correction due to m was added to ω . That correction was divided into the following two parts. The first part is the term, $-(m/2G)M_t$, which depends on the constituent mass M_t but not on the wave number q . This term lowers ω more markedly for the larger M_t , independently of q . Hence, this first part, $-(m/2G)M_t$, has possibility to tend to realize the spatially inhomogeneous chiral condensate. The second part is the term written as $(\delta\omega_D + \delta\omega_F)$, which depends on both M_t and q . According to numerical calculations, the value of $(\delta\omega_D + \delta\omega_F)$ at $q \neq 0$ is larger than that at $q = 0$ for each value of M_t . Therefore, the second part, $(\delta\omega_D + \delta\omega_F)$ tends not to realize the spatially inhomogeneous chiral condensate. Whether the introduction of the finite current mass tends to realize the spatially inhomogeneous chiral condensate or not depends on the competition between the term $-(m/2G)M_t$ and the term $(\delta\omega_D + \delta\omega_F)$.

The introduction of the current mass influences not only the possibility of the spatially inhomogeneous chiral condensate but also space dependence of the baryon number density. In the chiral limit, the baryon number density is spatially homogeneous even if the spatially inhomogeneous chiral condensate occurs [6, 7]. In contrast, when the current mass takes a finite value, the baryon number density becomes spatially inhomogeneous if the spatially inhomogeneous chiral condensate is realized. In addition, the wave number vector of the spatially inhomogeneous baryon number density coincides with that of the spatially inhomogeneous chiral condensate when the value of the current mass is small.

Here we give consideration to the ansatz Eq.(4) that describes the spatially inhomogeneous dual chiral condensate. In the chiral limit, the Lagrangian is chiral invariant and this ansatz seems to be appropriate because $\langle \bar{\psi}\psi \rangle$ and $\langle \bar{\psi}i\gamma_5\tau_3\psi \rangle$ are put on a chiral circle, $\langle \bar{\psi}\psi \rangle^2 + \langle \bar{\psi}i\gamma_5\tau_3\psi \rangle^2 = C^2$. On the other hand, when the current mass is finite, the Lagrangian is not chiral invariant and there might exist more appropriate ansatz than Eq.(4). In such ansatz, $\langle \bar{\psi}\psi \rangle$ and $\langle \bar{\psi}i\gamma_5\tau_3\psi \rangle$ are not put on the chiral circle and would satisfy more complicated relation. In the present paper dealing with the finite current mass, however, we have assumed the ansatz Eq.(4) for simplicity. Within the limits of this ansatz, we found the ground state with $M_t > 0$ and $q \neq 0$. Also, the baryon number density was found to be spatially inhomogeneous as well as the chiral condensate. If we can find more appropriate ansatz than Eq.(4), we would be

able to have thermodynamic potential whose minimum value is smaller than the minimum value obtained by use of the ansatz Eq.(4). With such more appropriate ansatz than Eq.(4), physical quantities such as the baryon number density will be affected and the way of the phase transition might be influenced. Besides our ansatz, other type of ansatz was studied in Ref [15, 20] as discussed in section 1. In order to determine which ansatz is to be realized, one needs to compare the thermodynamic potentials between them.

Several problems are still remained. First, it will be interesting to carry out numerical calculations with finite temperature $T > 0$. The phase diagram in the $T - \mu$ plane should be affected when the current quark mass is taken to be non-zero [15, 20]. Second, the study with the inclusion of color superconductivity. In the chiral limit, the phase diagram in the $T - \mu$ plane including a second color superconducting phase (2SC), uniform chiral and non-uniform chiral phase is studied [21]. The introduction of non-zero current quark mass should influence the diagram. Finally, in the NJL model with quark mass term there appears the Nambu-Goldstone boson (NG boson) when the ground state with spatially inhomogeneous chiral condensate is realized. Since this inhomogeneous chiral condensate breaks space translational symmetry spontaneously, the NG boson appears [22]. In the low energy phenomena, the NG boson would play an important role.

Acknowledgments

The author thanks the Yukawa Institute for Theoretical Physics at Kyoto University. Discussions during the YITP workshop YITP-W-08-09 on "Thermal Quantum Field Theories and Their Applications" were useful to complete this work.

Appendix

A Input parameters

We explain in this appendix a way to set the values of the input parameters (G, m, Λ) of the NJL model in the proper-time regularization (PTR) scheme. In the vacuum state $\mu = 0$, the pion decay constant f_π in the PTR scheme is represented as [4]

$$f_\pi^2 = \frac{N_c M_t^2}{4\pi^2} \int_{M_t^2/\Lambda^2}^{\infty} dt \frac{1}{t} e^{-t}, \quad (\text{A.1})$$

and the pion mass m_π satisfies the following relation [4],

$$m_\pi^2 f_\pi^2 = m \frac{1}{2G} M_t. \quad (\text{A.2})$$

The gap equation in the PTR scheme becomes [4]

$$M_t = m + \frac{1}{2\pi^2} G N_c N_f M_t F_2(M_t^2, \frac{1}{\Lambda^2}), \quad (\text{A.3})$$

where the function F_2 is defined as

$$F_2(M_t^2, \frac{1}{\Lambda^2}) \equiv \int_{1/\Lambda^2}^{\infty} ds \frac{1}{s^2} e^{-M_t^2 s} = \Lambda^2 \int_{M_t^2/\Lambda^2}^{\infty} dt \frac{1}{t^2} e^{-t}. \quad (\text{A.4})$$

Now, we give an arbitrary value to Λ firstly. Then, m and G are determined so as to reproduce the values $f_\pi = 92.4 \text{ MeV}$ and $m_\pi = 135 \text{ MeV}$. When the value of Λ is given, one can calculate the value of M_t through Eq.(A.1). Regarding the equations Eq.(A.2) and Eq.(A.3) as simultaneous equations for G and m , one can obtain both the values of G and m . Thus, we can determine the values of G and m for a given value of Λ .

B Chiral symmetry restoration and proper-time regularization

In this appendix, we look into the reason why the M_t becomes less than the current mass, $M_t < m$ for $q = 0$ and large chemical potential $\mu \gtrsim 0.7\Lambda$ in the numerical calculations. At the minimum point of the thermodynamic potential ω with $q = 0$ and $T = 0$, the condition, $\delta\omega/\delta M_t = 0$, is held,

$$M_t - m = 4G N_c N_f M_t \left[\frac{1}{8\pi^2} \int_{1/\Lambda^2}^{\infty} ds \frac{1}{s^2} \exp(-M_t^2 s) - \int \frac{d^3 p}{(2\pi)^3} \frac{1}{\epsilon} \theta(\mu - \epsilon) \right], \quad (\text{B.1})$$

where $\epsilon = \sqrt{\mathbf{p}^2 + M_t^2}$. This is nothing but the gap equation and it should be noted that the PTR scheme has been used in this equation. The first (second) term in the

brackets of Eq.(B.1) represents the contribution from the Dirac sea (Fermi sea). The second term increases if the chemical potential μ becomes larger. When the chemical potential reaches a certain value μ_c , the second term becomes equal to the first term,

$$\frac{1}{8\pi^2} \int_{1/\Lambda^2}^{\infty} ds \frac{1}{s^2} \exp(-M_t^2 s) = \int \frac{d^3 p}{(2\pi)^3} \frac{1}{\epsilon} \theta(\mu_c - \epsilon), \quad (\text{B.2})$$

and then one has $M_t = m$ from Eq.(B.1). If the chemical potential μ is larger than μ_c , the second term becomes larger than the first term and one has $M_t < m$. In short the relationship between M_t and m in terms of size is summarized as follows. For small values of the chemical potential μ , M_t is larger than m . When μ reaches μ_c , we have $M_t = m$. If μ becomes larger than μ_c , we have $M_t < m$. Now, let us estimate the value of μ_c assuming $M_t/\Lambda \ll 1$. The expansion of the left side of Eq.(B.2) about $M_t/\Lambda = 0$ takes the form [4]

$$\begin{aligned} \frac{1}{8\pi^2} \int_{1/\Lambda^2}^{\infty} ds \frac{1}{s^2} \exp(-M_t^2 s) &= \frac{\Lambda^2}{8\pi^2} \left(\frac{M_t^2}{\Lambda^2} \right) \int_{M_t^2/\Lambda^2}^{\infty} dt \frac{1}{t^2} \exp(-t) \\ &= \frac{\Lambda^2}{8\pi^2} \left[1 + (\gamma - 1) \left(\frac{M_t^2}{\Lambda^2} \right) + \dots \right]. \end{aligned} \quad (\text{B.3})$$

The expansion of the right side of Eq.(B.2) about $M_t/\Lambda = 0$ is

$$\frac{\Lambda^2}{4\pi^2} \left[\left(\frac{\mu_c^2}{\Lambda^2} \right) - \frac{1}{2} \left(\frac{M_t^2}{\Lambda^2} \right) + \dots \right]. \quad (\text{B.4})$$

Neglecting the order $O(M_t^2/\Lambda^2)$ in Eq.(B.2), we have

$$\mu_c \approx \frac{\Lambda}{\sqrt{2}} \approx 0.7\Lambda. \quad (\text{B.5})$$

Thus, we can understand roughly why M_t becomes less than m for $\mu \gtrsim 0.7\Lambda$ in the PTR scheme.

It would be helpful to examine the relationship between M_t and m in a different regularization scheme, say the three-momentum cut-off scheme [4]. In this scheme, the first term in the brackets of the gap equation Eq.(B.1) is replaced by

$$\int \frac{d^3 p}{(2\pi)^3} \frac{1}{\epsilon} \theta(\Lambda_{3\text{-momentum}} - |\mathbf{p}|). \quad (\text{B.6})$$

The value of the chemical potential at which the equation enclosed in brackets of the gap equation becomes zero is

$$(\mu_c)_{3\text{-momentum}} \approx \Lambda_{3\text{-momentum}}. \quad (\text{B.7})$$

Therefore, M_t does not become less than m for $\mu \lesssim \Lambda_{3\text{-momentum}}$ in the three-momentum cut-off scheme.

References

- [1] B. C. Barrois, Nucl. Phys. B 129 (1977), 390.
- [2] D. Bailin and A. Love, Phys. Rep. 107 (1984), 325.
- [3] Y. Nambu and G. Jona-Lasinio, Phys. Rev. 122 (1961), 345.
- [4] For a review, see S. P. Klevansky, Rev. Mod. Phys. 64 (1992), 649.
- [5] For a review, see M. Buballa, Phys. Rep. 407 (2005), 205.
- [6] T. Tatsumi and E. Nakano, hep-ph/0408294.
- [7] E. Nakano and T. Tatsumi, Phys. Rev. D 71 (2005), 114006.
- [8] D. V. Deryagin, D. Yu. Grigoriev, and V. A. Rubakov, Int. J. Mod. Phys. A 7 (1992), 659.
- [9] A. W. Overhauser, Phys. Rev. 128 (1962), 1437.
- [10] E. Shuster and D. T. Son, Nucl. Phys. B 573 (2000), 434.
- [11] B.-Y. Park, M. Rho, A. Wirzba, and I. Zahed, Phys. Rev. D 62 (2000), 034015.
- [12] R. Rapp, E. Shuryak, and I. Zahed, Phys. Rev. D 63 (2001), 034008.
- [13] V. Schön and M. Thies, Phys. Rev. D 62 (2000), 096002.
- [14] K. Ohwa, Phys. Rev. D 65 (2002), 085040.
- [15] D. Nickel, Phys. Rev. D 80 (2009), 074025, arXiv:0906.5295 [hep-ph].
- [16] J. I. Kapusta, *Finite-Temperature Field Theory* (Cambridge University Press, Cambridge, England, 1989).
- [17] S. Maedan, Prog. Theor. Phys. 118 (2007), 729.
- [18] J. Schwinger, Phys. Rev. 82 (1951), 664.
- [19] M. Asakawa and K. Yazaki, Nucl. Phys. A 504 (1989), 668.
- [20] D. Nickel, Phys. Rev. Lett. 103 (2009), 072301, arXiv:0902.1778 [hep-ph].
- [21] M. Sadzikowski, Phys. Lett. B 642 (2006), 238.
- [22] R. Casalbuoni and G. Nardulli, Rev. Mod. Phys. 76 (2004), 263.